Improved Hybrid Method to Calculate Inductances of Permanent Magnet Synchronous Machines with Skewed Stators Based on Winding Function Theory

Yuting Gao, Ronghai Qu, and Dawei Li*

(State Key Laboratory of Advanced Electromagnetic Engineering and Technology, School of Electrical and Electronic Engineering, Huazhong University of Science and Technology, Wuhan 430074, China)

Abstract: An improved hybrid method combining two dimensional (2D) finite element analysis (FEA) and the analytical method is put forward to calculate the stator winding inductance and synchronous inductance influenced by stator skewing technique. Based on winding function theory (WFT), the improved method proposes two factors to describe variable inductances along the stator skewing angles. Comprehensive simulations are then performed on three interior permanent magnet synchronous machines (IPMSMs), one normal and two skewed machines (half slot and one slot pitch skewing respectively). Extensive experiments are conducted on relevant prototypes with good correlation. Moreover, analysis and comparisons are made as to the influence of different skewing angles on the inductances and torque-speed curves. It is found that L_d increases and L_q decreases by skewing, leading to the reduction of the rotor saliency and maximal torque capability, but increase of the flux weakening capability.

Keywords: Finite element analysis(FEA), inductances, permanent magnet synchronous machine (PMSM), skewing, winding function theory (WFT).

Nomenclature

φ Angular position of d-axis with respect to the axis of phase a.
θ Particular position in the stator reference frame measured from the axis of phase a.
$N(\theta)$ Winding function.
r Average radius of air-gap.
g^{-1} Air-gap inverse function.
l Active stack length.
N Total turns per phase.
p Number of pole pairs.
α_e Electrical skewing angle.
K_{dh} h^{th} harmonic distribution factor.
K_{ph} h^{th} harmonic pitch factor.
K_{sh} h^{th} harmonic skewing factor.
K_{s1} 1^{st} harmonic skewing factor.
L_{aa}^{2D} Self-inductance of phase a without skewing.
M_{ac}^{2D} Mutual-inductance between phase a and c without skewing.
L_{aa}^{sk} Self-inductance of phase a with skewing.
M_{ac}^{sk} Mutual-inductance between phase a and c with skewing.
L_d^{2D} d-axis synchronous inductance without skewing.
L_q^{2D} q-axis synchronous inductance without skewing.
L_d^{sk} d-axis synchronous inductance with skewing.
L_q^{sk} q-axis synchronous inductance with skewing.
β Angle between the phase a axis of different slice and the unskewed phase a axis.
L_e End winding inductance.
Ψ_m Flux linkage produced by permanent magnets.
γ Angle which the stator current (MMF) leads the q-axis.

1 Introduction

Permanent magnet synchronous machines (PMSMs) exhibit advantages of high torque density, high efficiency and easy maintenance, thus being employed in many civil and industry applications[1-4]. The stator's winding and synchronous inductances have great influence on both the steady-state and dynamic performance indexes of PMSMs, such as torque ability, flux-weakening capabilities, rotor position estimation, etc[5-7]. However, when stator skewing technique is employed to improve the electromagnetic performances (e.g. to achieve sinusoidal waveforms of back electromotive force (EMF) and air-gap flux density[8-10], and to decrease cogging torque and torque ripple[11-14]), two dimensional(2D) finite element analysis (FEA) cannot take skewing effect into account effectively because it cannot describe any change of flux density along the axial direction[15-16]. In order to get more accurate inductances, three dimensional(3D) FEA should be introduced to the skewing PMSMs, but its simulation time is very long for numerous meshes. Even worse, the 3D model may not converge if the boundary conditions are not aligned correctly.

In order to get a good balance between computational time and calculation accuracy, a hybrid of 2D FEA and analytical method has been introduced in [17] to predict the winding inductances, L_d and L_q with

* Corresponding Author, E-mail: ronghaiqu@hust.edu.cn.
Supported by National Natural Science Foundation of China under Grant 51520105010.

skewing, regardless of the influence of cross-coupling. An improved analytical method has then been developed to calculate L_d and L_q, taking both skewing and cross-coupling effect into consideration[18]. These two papers separate the active length of the skewed machine into many slices along the axial direction as shown in Fig.1, of which each slice can be regarded as an unskewed 2D slice. Afterwards, the inductances of every slice are computed independently, and then integrated together to get the total inductance. From Fig.2, it can be seen that the stator's self- and mutual-inductances, and synchronous inductances of different 2D slices vary with the axial position. This is because the angular position with respect to *d*-axis is different for each slice. However, the variations of the inductances have not been considered in these papers, which cannot be neglected when the electrical skewing angle is relatively big or slot per phase per pole is small.

An improved hybrid method combining 2D FEA and numerical circuit model to calculate the stator self-, mutual- and synchronous inductances is proposed in this paper, which take the variation of the inductances with the axial position into consideration. In order to describe the inductances accurately when affected by variable magnetic resistance, this paper divides the machine into several pieces along the axial direction, and employs winding function theory (WFT) to study the skewing influence. It then puts forward two coefficients to modify the mathematical equations for different inductances[19-23]. This paper is organized as follows. Section 2 presents the basic principles and formulas to calculate the inductances with skewed stators. Many FEA simulations and experiments are conducted in Section 3 on three PMSMs, including one normal and two skewed machines (half slot and one slot pitch skewing respectively)[24], where lots of comparisons and analysis have been done. Conclusions are drawn in Section 4.

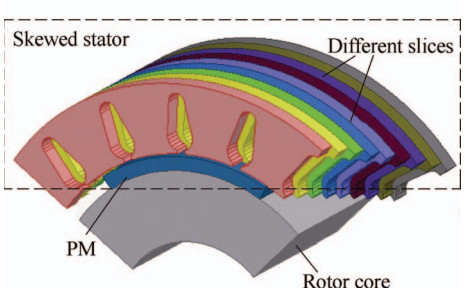

Fig.1 Separated 2D slices of the skewed machine

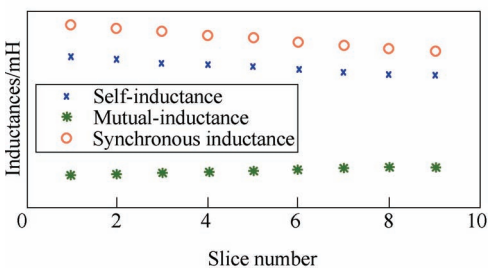

Fig.2 Self- and mutual-inductances of different slices

2 Improved method to calculate inductances with skewing stators

In order to simplify the inductance calculation, some assumptions are made as follows:

1) Stator is smooth, i.e. regardless of slot opening effect.

2) The leakage inductance is not influenced by skewing effect.

The general expression for stator inductances between any two phases i and j, neglecting of saturation, can be calculated by WFT as follows:

$$L_{ij}(\varphi)=\mu_0 rl\int_0^{2\pi} g^{-1}(\varphi,\theta)N_i(\theta)N_j(\theta)\mathrm{d}\theta \tag{1}$$

where $N_i(\theta)$ and $N_j(\theta)$ are winding functions of phase i and j respectively. The definitions of angle φ and θ are expressed in stator reference frame, described in Fig.3. It is known that the phase winding consists of coils, and hence the phase winding function in (1) can be obtained by summing each coil winding functions together. For example, the winding function of concentrated coil k, as shown in Fig.4, whose sides are placed at θ=0 and θ=π, is defined by

$$N_k(\theta)=\begin{cases} n/2 & 0\leqslant\theta\leqslant\pi \\ -n/2 & \pi<\theta<2\pi \end{cases} \tag{2}$$

where n is the total number of turns of coil k. The Fourier series of the rectangular wave is

$$N_k(\theta)=\frac{4}{\pi}\frac{n}{2}(\sin\theta+\sin 3\theta+\sin 5\theta+\cdots) \tag{3}$$

Then it is easy to deduce the winding function for a specific winding layout for PMSMs. For conventional distributed fractional pitch windings without skewing, the circuit winding function can be described as

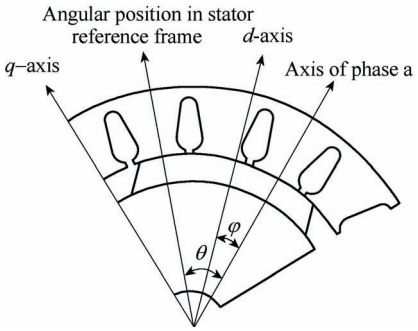

Fig.3 Definition of different angles

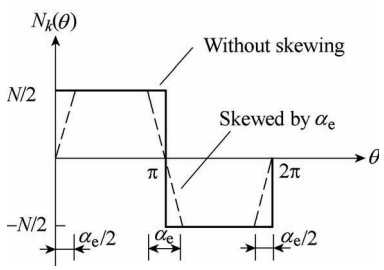

Fig.4 Winding function of concentrated coil k

$$N(\theta)=\frac{4}{\pi}\frac{N}{2p}\sum_{h=1,3,5}^{\infty}\frac{K_{dh}K_{ph}}{h}\sin(h\theta) \tag{4}$$

Generally, the air-gap inverse function for any type of PMSMs can be written in the following Fourier series form:

$$g^{-1}(\varphi,\theta)=\delta_0+\sum_{m=2,4,6}^{\infty}\delta_m\cos[m(\theta-\varphi)] \tag{5}$$

For simplification of the calculation, it can be approximated by the first two terms, as illustrated by

$$g^{-1}(\varphi,\theta)\approx\delta_0+\delta_2\cos[2(\theta-\varphi)] \tag{6}$$

Substituting (4) and (6) into (1), the stator winding inductances can be worked out as

$$L_{aa}=L_l+L_0+L_2\cos 2\varphi \tag{7}$$

$$M_{ac}=M_0+M_2\cos 2\left(\varphi-\frac{2\pi}{3}\right) \tag{8}$$

where L_l is the additional leakage flux component, L_0 and M_0 are the components of self- and mutual-inductances due to the space-fundamental air-gap flux, L_2 and M_2 are the second harmonic components of self- and mutual-inductances resulted from the saliency of rotor. The self-inductances of phase b and phase c are identical with (7) except for displacement by 2π/3 and 4π/3 respectively. The mutual-inductances of a&b and b&c are also the same with (8) but shifted by 2π/3 and 4π/3 respectively. The inductances of surface-mounted PMSM (SPMSM) do not have the last term in (7) and (8) due to the non-saliency of rotor.

It should be noted that the above derivations are made without skewing structure. However, when the coil is skewed by angle α_e, the circuit winding functions and angular positions of windings will change, thus having a great effect on the inductance values. As the air-gap inverse function is different between SPMSM and interior PMSM (IPMSM), the influence of skewing on their inductances will be investigated separately.

2.1 Influence of skewing on the inductances of SPMSM

In Fig.4, the changes of winding function for coil k with skewing can be observed in details (from rectangular wave to trapezoidal wave). The Fourier series of the trapezoidal wave can be given as

$$N_k^{sk}(\theta)=\frac{4}{\pi}\frac{N}{2}\left[\frac{\sin\alpha_e/2}{\alpha_e/2}\sin\theta+\frac{\sin 3\alpha_e/2}{3\alpha_e/2}\sin 3\theta+\frac{\sin 5\alpha_e/2}{5\alpha_e/2}\sin 5\theta+\cdots\right] \tag{9}$$

where the superscript sk denotes the machine with skewing. Hence, the circuit winding function can be derived as

$$N^{sk}(\theta)=\frac{4}{\pi}\frac{N}{2p}\sum_{h=1,3,5}^{\infty}\frac{K_{dh}K_{ph}}{h}K_{sh}\sin(h\theta) \tag{10}$$

where the h^{th} harmonic skew factor K_{sh} is given by

$$K_{sh}=\frac{\sin(h\alpha_e/2)}{h\alpha_e/2} \tag{11}$$

Before proceeding to the calculation of inductances, it is essential to investigate whether other parameters in (1) could change due to the effect of skewing. For SPMSM, the permanent magnets are mounted on the surface of rotor and the permeability of PM is very close to air, so the air-gap inverse function g^{-1} is independent of rotor angle. Moreover, the skewing does not affect the air-gap length because the air-gap lengths of every part are identical to each other, when the machine is divided into several segments in the axial direction. Therefore, after substituting (10) into (1), the skewed stator inductances can be finally written as

$$L_{aa}^{sk}=\sum_{h=1,3,5}^{\infty}K_{sh}^2L_{aa}^{2D} \tag{12}$$

$$M_{ac}^{sk}=\sum_{h=1,3,5}^{\infty}K_{sh}^2M_{ac}^{2D} \tag{13}$$

where L_{aa}^{2D} and M_{ac}^{2D} can be obtained through 2D FEA model without skewing. If 3rd, 5th ⋯ harmonics are negligible, Eqs (12) and (13) can be approximated by

$$L_{aa}^{sk}\approx K_{s1}^2L_{aa}^{2D} \tag{14}$$

$$M_{ac}^{sk}\approx K_{s1}^2M_{ac}^{2D} \tag{15}$$

where K_{s1} is the first harmonic skew factor, as expressed by

$$K_{s1}=\frac{\sin(\alpha_e/2)}{\alpha_e/2} \tag{16}$$

The self- and mutual-inductances of phase b and c have the similar relations as (14) and (15) respectively. With the help of Park transformation, the relationship between synchronous and stator winding inductances of SPMPM can be described as[14]

$$L_d^{2D}=L_q^{2D}=L_{aa}^{2D}+M_{ac}^{2D} \tag{17}$$

Then the synchronous inductance of the skewed SPMSM can be obtained by

$$L_{d(q)}^{sk}=L_{aa}^{sk}+M_{ac}^{sk}\approx K_{s1}^2L_{aa}^{2D}+K_{s1}^2M_{ac}^{2D} \tag{18}$$

Therefore, the relationship between synchronous inductance with and without skewing is

$$L_{d(q)}^{sk}\approx K_{s1}^2L_{d(q)}^{2D}=\left(\frac{\sin\alpha_e/2}{\alpha_e/2}\right)^2L_{d(q)}^{2D} \tag{19}$$

As aforementioned, once L_{aa}^{2D}, M_{ac}^{2D} and $L_{d(q)}^{2D}$ have been deduced from 2D FEA, the inductances considering skewing are able to be worked out through (14), (15) and (19) respectively.

2.2 Influence of skewing on the inductances of IPMSM

The air-gap length of IPMSM is non uniform due to the rotor saliency. When the skewing technique is applied, the active length of the machine will be subdivided into several 2D slices, and the angular position of *d*-axis with respect to phase a winding of different 2D slices is varied in the axial direction. Meanwhile, the axis of the phase a winding for each slice with respect to the unskewed phase a axis could also be changed. Therefore, the self-inductance of phase a is given as

$$L_{\mathrm{aa}}^{\mathrm{sk}}=\mu_0 rl\int_{-\alpha_{\mathrm{e}}/2}^{\alpha_{\mathrm{e}}/2}\int_0^{2\pi}(\delta_0+\delta_2\cos 2(\theta-(\varphi+\beta)))\times \frac{1}{\alpha_{\mathrm{e}}}\frac{4}{\pi}\frac{N}{2p}\sum_{h=1,3,5}^{\infty}\frac{K_{\mathrm{d}h}K_{\mathrm{p}h}}{h}\sin(h(\theta+\beta))\mathrm{d}\theta\mathrm{d}\beta \quad (20)$$

After simplification of (20) and careful comparison with (7), the influence of skewing on self-inductance can then be summarized as

$$L_{\mathrm{aa}}^{\mathrm{sk}}=L_l+\left(\frac{\sin\alpha_{\mathrm{e}}/2}{\alpha_{\mathrm{e}}/2}\right)^2 L_0^{2\mathrm{D}}+\left(\frac{\sin\alpha_{\mathrm{e}}/2}{\alpha_{\mathrm{e}}/2}\right)^2\left(\frac{\sin\alpha_{\mathrm{e}}}{\alpha_{\mathrm{e}}}\right)L_2^{2\mathrm{D}}\cos 2\varphi$$

$$=L_l+K_{\mathrm{s1}}^2L_0^{2\mathrm{D}}+K_{\mathrm{s1}}^2K_\alpha L_2^{2\mathrm{D}}\cos 2\varphi \quad (21)$$

Similarly, the skewed mutual-inductance between phases a and c can be expressed as

$$M_{\mathrm{ac}}^{\mathrm{sk}}=K_{\mathrm{s1}}^2M_0^{2D}+K_{\mathrm{s1}}^2K_\alpha M_2^{2\mathrm{D}}\cos 2\left(\varphi-\frac{2}{3}\pi\right) \quad (22)$$

where K_α is a coefficient defined by

$$K_\alpha=\frac{\sin\alpha_{\mathrm{e}}}{\alpha_{\mathrm{e}}} \quad (23)$$

The $L_0^{2\mathrm{D}}$, $M_0^{2\mathrm{D}}$, $L_2^{2\mathrm{D}}$ and $M_2^{2\mathrm{D}}$ can be calculated using 2D FEA. L_l is so small that the skewing effect can be considered as negligible. The self-inductances of phase b and c are identical with (21) but displaced by 2π/3 and 4π/3 respectively. The mutual-inductances of phase a&b and phase b&c are also the same as those of (22) but shifted by 2π/3 and 4π/3 respectively. Since SPMSM does not have the last term in (21) and (22), (14) and (15) can be regarded as a particular case of (21) and (22) respectively.

In general, based on Park transformation, the relationship between the components of stator self- and mutual-inductances, and the *d*- and *q*-axis inductances, are given by [26]

$$L_d^{2\mathrm{D}}=L_l+(L_0^{2\mathrm{D}}-M_0^{2\mathrm{D}})+\left(\frac{L_2^{2\mathrm{D}}}{2}+M_2^{2\mathrm{D}}\right) \quad (24)$$

$$L_q^{2\mathrm{D}}=L_l+(L_0^{2\mathrm{D}}-M_0^{2\mathrm{D}})-\left(\frac{L_2^{2\mathrm{D}}}{2}+M_2^{2\mathrm{D}}\right) \quad (25)$$

So the *d*- and *q*-axis inductances, considering skewing can be obtained as

$$L_d^{\mathrm{sk}}=L_l+K_{\mathrm{s1}}^2(L_0^{2\mathrm{D}}-M_0^{2\mathrm{D}})+K_{\mathrm{s1}}^2K_\alpha\left(\frac{L_2^{2\mathrm{D}}}{2}+M_2^{2\mathrm{D}}\right) \quad (26)$$

$$L_q^{\mathrm{sk}}=L_l+K_{\mathrm{s1}}^2(L_0^{2\mathrm{D}}-M_0^{2\mathrm{D}})-K_{\mathrm{s1}}^2K_\alpha\left(\frac{L_2^{2\mathrm{D}}}{2}+M_2^{2\mathrm{D}}\right) \quad (27)$$

Thus, from (24) to (27), the relationship between the inductances $L_d^{2\mathrm{D}}$ and $L_q^{2\mathrm{D}}$, which can be deduced from 2D FEA of the cross section of a machine without skewing, and the inductances L_d^{sk} and L_q^{sk}, considering skewing, are derived as

$$L_d^{\mathrm{sk}}=K_{\mathrm{s1}}^2L_d^{2\mathrm{D}}+\frac{1-K_\alpha}{2}(L_q^{2\mathrm{D}}-L_d^{2\mathrm{D}})K_{\mathrm{s1}}^2 \quad (28)$$

$$L_q^{\mathrm{sk}}=K_{\mathrm{s1}}^2L_q^{2\mathrm{D}}-\frac{1-K_\alpha}{2}(L_q^{2\mathrm{D}}-L_d^{2\mathrm{D}})K_{\mathrm{s1}}^2 \quad (29)$$

Therefore, as mentioned above, after 2D FEA calculations of stator winding and synchronous inductances, Eqns. (21), (22), (28) and (29) can be employed to deduce the inductances with skewing.

At last, the end winding inductance L_{e} can be estimated by the analytical technique proposed in [27] which is widely applied in AC machines. Then, the synchronous inductances are given as

$$L_d=L_d^{\mathrm{sk}}+L_{\mathrm{e}} \quad (30)$$

$$L_q=L_q^{\mathrm{sk}}+L_{\mathrm{e}} \quad (31)$$

where L_d and L_q are *d*- and *q*-axis inductances considering stator skewing and end effects.

2.3 Influence of skewing on torque-speed curves

The torque-speed curve is one of the key performance indexes for PMSMs. In this part, lots of investigations are made to find any stator skewing influence on torque-speed curve. By the fundamental principle of PMSMs, the electromagnetic torque can be estimated by

$$T_{\mathrm{em}}=p[\psi_{\mathrm{m}}i_q+(L_d-L_q)i_di_q] \quad (32)$$

The skewed machine can be subdivided into several slices along the axial direction. For each slice, the flux linkages Ψ_{m} produced by PMs are identical with each other. However, the *d*- and *q*-axis currents of different slices will not be the same, which can be observed in Fig.5 in detail. Then the electromagnetic torque can be deduced by

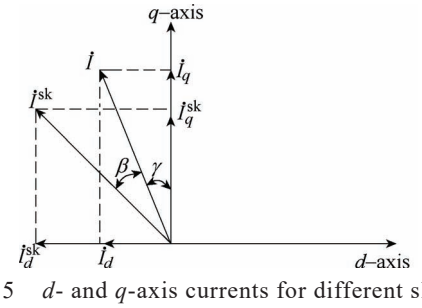

Fig.5 *d*- and *q*-axis currents for different slices

$$T_{\mathrm{em}}^{*}=\frac{1}{\alpha_{\mathrm{e}}}\int_{-\alpha_{\mathrm{e}}/2}^{\alpha_{\mathrm{e}}/2}\psi_{\mathrm{m}}^{*}I^{*}\cos(\beta+\gamma)+(L_{d}^{*}-L_{q}^{*})I^{*}\sin(\beta+\gamma)\cdot I^{*}\cos(\beta+\gamma)\mathrm{d}\beta$$
$$=I^{*}K_{\mathrm{s1}}\cos\gamma+I^{*2}K_{\alpha}\frac{L_{d}^{\mathrm{sk}*}-L_{q}^{\mathrm{sk}*}}{2}\sin 2\gamma \qquad (33)$$

where the superscript * means per unit. From (33), it can be found that the torque capability is determined not only by the skewing angles, but also by the stator current.

3 Simulations and experiments

Firstly, the predicted stator self-, mutual- and synchronous inductances of the improved hybrid method are compared with the results of 3D FEA simulations. Then, comprehensive experimental validations are made. Since SPMSM can be viewed as a special case of IPMSM whose saliency ratio is equal to 1, relevant validations are conducted on three 35kW IPMSMs. The only difference among these prototypes is skewing angle, i.e. model I without skewing, model II with half slot pitch skewing and model III with one slot pitch skewing. The detailed specifications are summarized in Table 1.

Table 1 Specifications of the IPMSMs

Item	Model I	Model II	Model III
Skewing	No skewing	Half slot pitch	One slot pitch
Power/kW	35		
No. of poles	6		
No. of slots	36		
Stator outer diameter/mm	240		
Air gap length/mm	1		
Core length/mm	80		
PM thickness/mm	8		
PM length/mm	27		

3.1 Simulations by the improved hybrid method and 3D FEA

Firstly, the stator self- and mutual-inductances are predicted using the hybrid method. Fig.6 shows the 2D FEA simulated stator self- and mutual-inductances at rated current of model I without skewing. The L_{aa} and M_{ac} values are plotted against rotor position. Then the $L_0^{2\mathrm{D}}$, $M_0^{2\mathrm{D}}$, $L_0^{2\mathrm{D}}$ and $M_0^{2\mathrm{D}}$ in (21) and (22) can be determined from curves. Hence, the skewed self- and mutual-inductances of model II and model III can be predicted, when (21) and (22) are employed respectively, just as shown in Figs.7 and 8 respectively. Meanwhile, the predicted values of the hybrid method are compared with 3D FEA results. Next, verifications for skewed synchronous inductances are conducted as well. The $L_d^{2\mathrm{D}}$ and $L_q^{2\mathrm{D}}$ for 2D machine is shown in Fig.9. Then, by applying (28) and (29), the values of L_d^{sk} and L_q^{sk} with different skewing angles can be determined, and the predicted synchronous inductances of model II and model III are compared carefully by 3D FEA as shown in Figs.10 and 11 respectively. From Figs. 6, 7, 9 and 10,

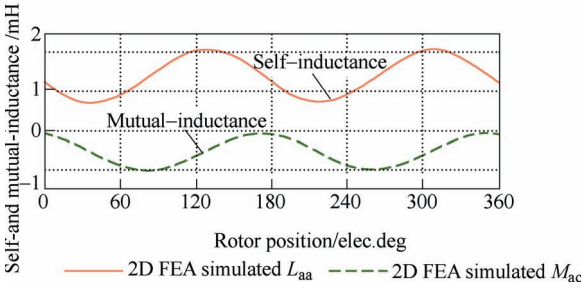

Fig.6 2D FEA results of stator self- and mutual-inductance of model I without skewing

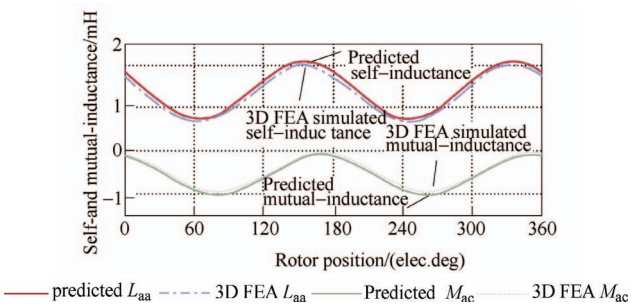

Fig.7 Stator self- and mutual-inductance of model II with half slot pitch skewing

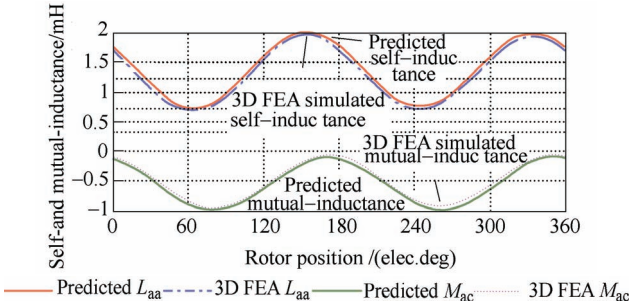

Fig.8 Stator's self- and mutual-inductances of model III with one slot pitch skewing

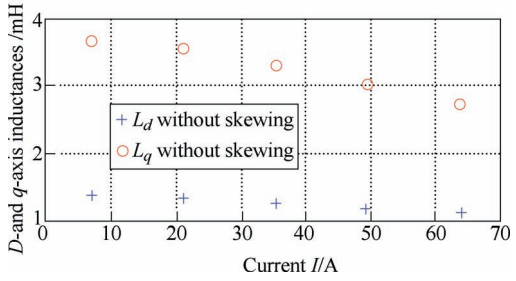

Fig.9 2D FEA results of *d*- and *q*-axis inductances of model I without skewing

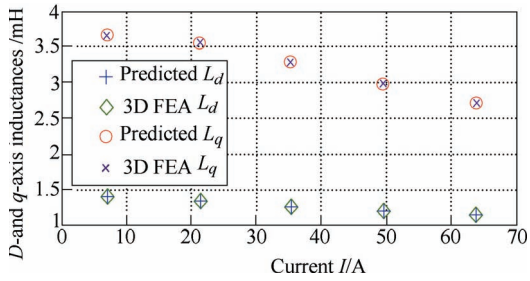

Fig.10 *d*- and *q*-axis inductances of model II with half slot pitch skewing

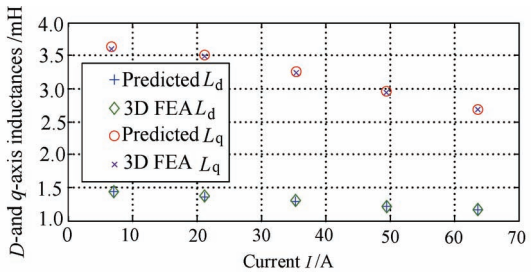

Fig.11 *d*- and *q*-axis inductances of model III with one slot pitch skewing

it can be found that good correlation has been achieved through the result comparisons, which demonstrates that the improved hybrid method is accurate and reliable. Moreover, the simulation time of the proposed method is much shorter than that of 3D FEA, shown in Table 2.

3.2 Experimental validations

Fig.13 shows the measured stator self- and mutual-inductances at rated current of model I without skewing using an ac standstill test method[24]. The voltage and current for various rotor positions are recorded using Agilent Infinii Vision 2000X, and a specifically designed device is used to detect rotor positions whose recognition accuracy is 0.5 degree. It also functions as a clamping mechanism to lock the rotor. The L_{aa} and M_{ac} values are plotted against rotor position, and the least-square curve fitting technique is applied to obtain the fitted curves. The parameters L_l+L_0, M_0, L_1 and M_1 without skewing can then be determined from the curve fittings. Hence, the self- and mutual-inductances of model II and model III can be predicted based on (21) and (22), respectively. The predicted self- and mutual-inductances are then validated by experiments. The L_{aa} and M_{ac} are tested every 5 mechanical degrees, and the fitted curves of the measured value can then be plotted. The comparisons between the measured and predicted inductances of model II are made in Fig.14, followed by model III in Fig.15. It can be seen that good agreements have been achieved. Moreover, the self-inductances are positive while the mutual-inductances are negative throughout the whole range of rotor position. This is because the axis of phase a with respect to phase c is 120 elec. degrees, and as a result the positive phase a current will result in positive flux linkage in phase a winding but negative in phase c winding. In addition, it can also be found that, the dc term of self-inductance curve is almost two times as that of the mutual-inductance curve, since the MMF excited by the phase a winding will become half after the projection on the phase c axis.

Table 2 Simulation time comparison

Method	Stator self- and mutual-inductance calculation	*d*- and *q*-axis inductance calculation
Improved hybrid method/min	30	25
3D FEA/h	9	8

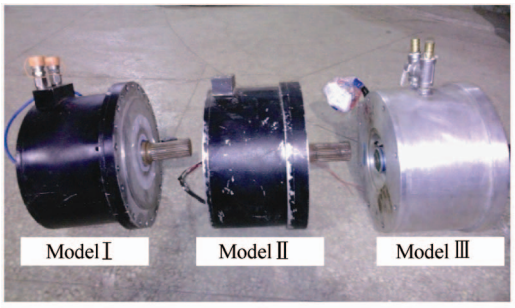

Fig.12 Three prototypes with different skewing angles

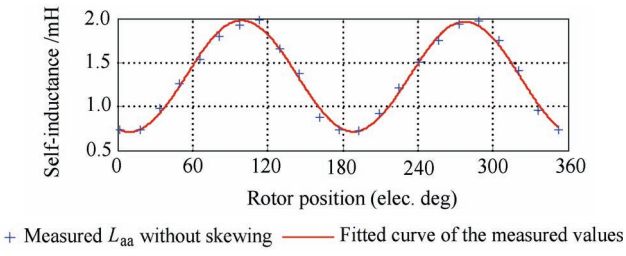

(a) Self-inductance

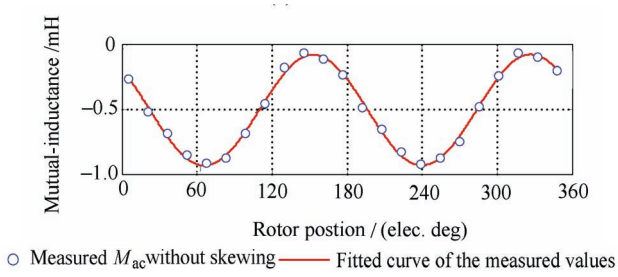

(b) Mutual-inductance

Fig.13 Stator's self- and mutual-inductances at rated current of model I without skewing

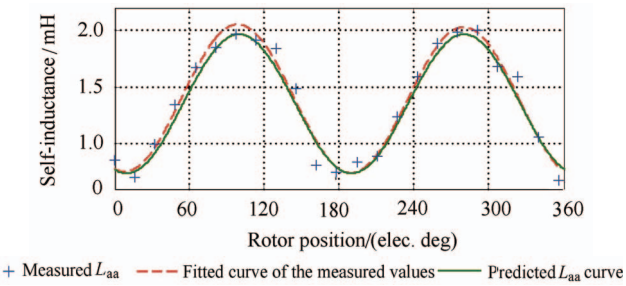

(a) Self-inductance

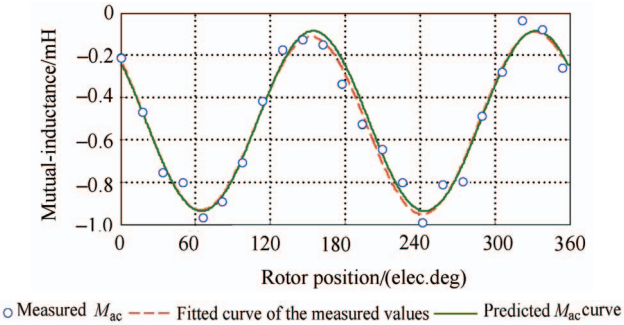

(b) Mutual-inductance

Fig.14 Stator self- and mutual-inductances at rated current of model II

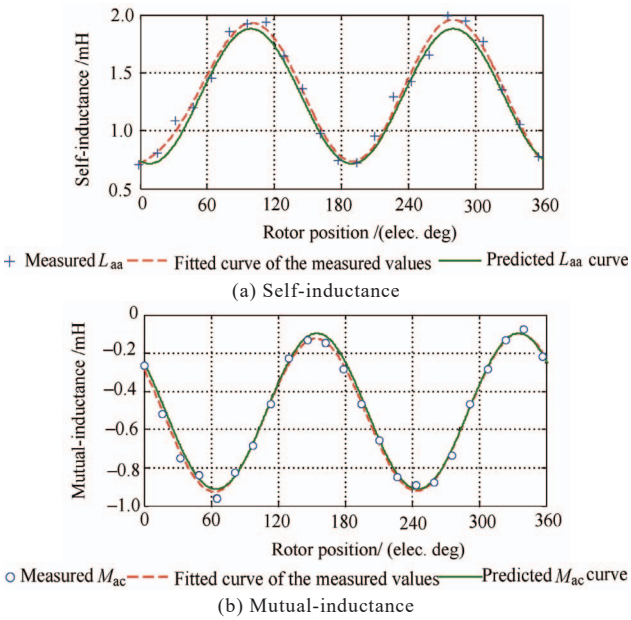

(a) Self-inductance

(b) Mutual-inductance

Fig.15 Stator self- and mutual-inductances at rated current of model III

Verifications of the prediction for skewed synchronous inductances are conducted as well. The d-axis inductances are measured by locking the rotor at the position where q-axis is aligned with phase a axis, then applying I_a=0, I_b=I_d and I_c=$-I_d$, and measuring the line voltage of terminal b&c. Meanwhile, the q-axis inductances are measured similarly by locking the rotor at the position where d-axis is aligned with phase a axis, and applying I_a=0, I_b=I_q and I_c=$-I_q$, then measuring the line voltage of terminal b&c. The measured L_d and L_q of model I without skewing are presented in Fig.16. Then by applying (28) and (29), the L_d^{sk} and L_q^{sk} value of different skewing angles can be determined. Figs.17 and 18 compare the measured and predicted synchronous inductances of model II and model III respectively. From Figs.16 to 18, the influence of saturation effect can be carefully observed. As the current increases, more saturated the iron part will be, hence the lower permeability of the flux path will lead to the decrease of synchronous inductance. Also, it can be found that L_q goes down much faster than L_d. This is because the q-axis magnetic field has a higher degree of saturation than that of the d-axis. So saturation effect has a larger impact on L_q.

As can be observed from Figs.13 to 18, good agreements have generally been achieved based on the new method, while some small errors might be attributed by the following factors:

(1) The rotor positioning error during the test would lead to the inaccuracy of the inductances. Since electrical angle is p times of mechanical angle, a small deviation will result in a relatively large orientation error.

(2) There are 4th, 6th… harmonics in stator winding inductances in practice, and the neglect may bring some error between simulation and measurement.

(3) The stator is assumed to be ideally smooth in the derivations, while it is not the case in the prototypes.

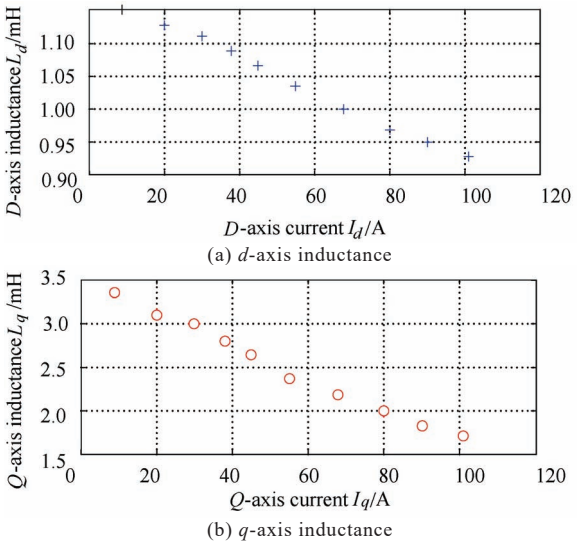

(a) d-axis inductance

(b) q-axis inductance

Fig.16 Measured d- and q-axis inductances of model I without skewing

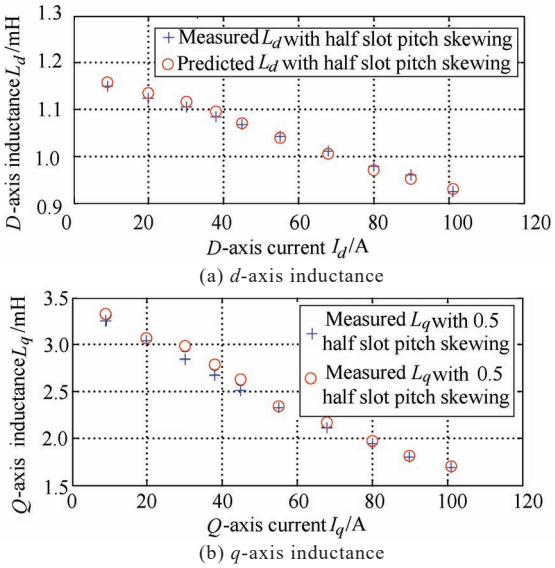

(a) d-axis inductance

(b) q-axis inductance

Fig.17 Measured and predicted d- and q-axis inductances of model II

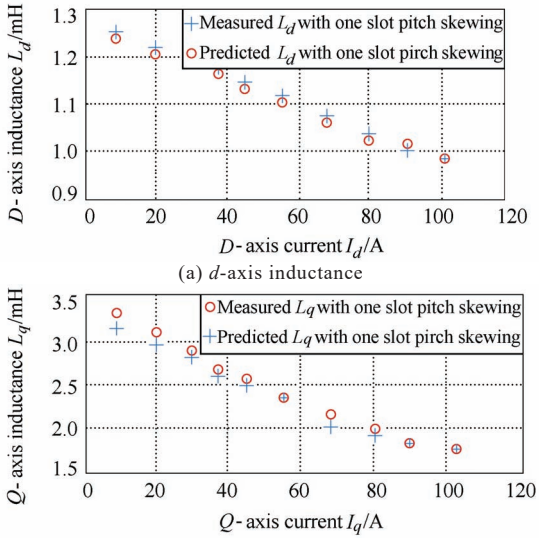

(a) d-axis inductance

(b) q-axis inductance

Fig.18 Measured and predicted d- and q-axis inductances of model III

Fig.19 investigates the influence of skewing on the *d*- and *q*-axis inductances, one without skewing and the other two with half and one slot pitch skewing respectively. It is evident that L_d increases as an effect of skewing, while L_q decreases gradually. This can be mathematically explained by (28) and (29). And from a physical standpoint, Fig.20(a) compares the measured flux linkage of the skewed and unskewed

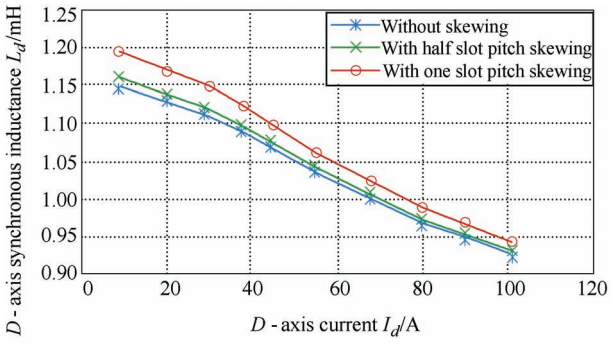

(a) *d*-axis inductance

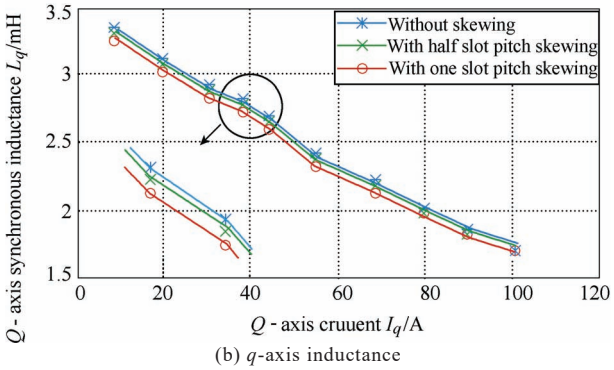

(b) *q*-axis inductance

Fig.19 *d*- and *q*-axis inductances with and without skewing

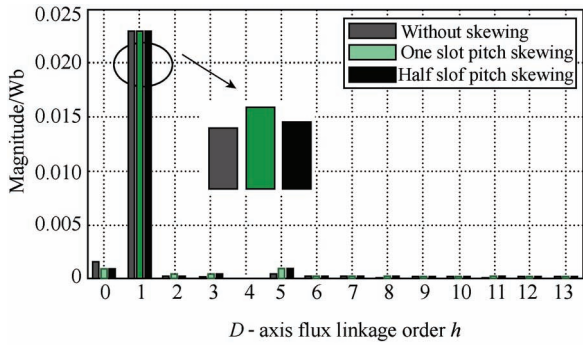

(a) *d*-axis flux linkage

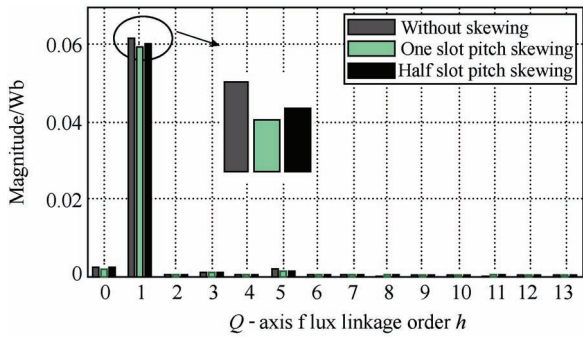

(b) *q*-axis flux linkage

Fig.20 *d*- and *q*-axis flux linkage of different skewing angles

machines when current 20A is applied to *d*-axis. From this figure, it can be noted that the *d*-axis inductance, which is the ratio of the flux linkage and current, becomes bigger when skewing is employed. Similar change for L_q can be seen in Fig.20(b) as well. Moreover, it is realized that the bigger the skewing angle is, the larger L_d is, and the smaller L_q is, resulting in reduction of rotor saliency. With regards to SPMSM, it is noted that the synchronous inductance $L_{d(q)}$ could decrease due to the skewing effect.

Fig.21 investigates the torque-speed curves of the three prototypes applied in EV application. It can be observed that, as the skewing angle goes up, the torque in constant power region will become smaller, while the flux weakening capability will become stronger. As the skewing angle increases, the detailed change of other parameters in (33) is given in Table 3. It is seen that in the constant power region, I^* is kept as a constant which is sometimes equal to 1. The electromagnetic torque is dominated by the first term in (33), thus it would decrease when skewing is employed. Then, in the flux weakening region, I^* drops and γ increases significantly in order to meet the limitation of dc-link voltage. Therefore, the second term, playing an important role in the flux weakening capabilities, is increased as the skewing angle becomes bigger. It should be noted that for different configurations or control algorithms, the variation tendency of torque characteristics may differ for different skewing angles and stator currents.

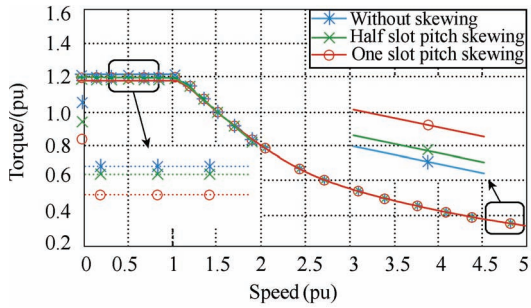

Fig.21 Torque-speed curves with and without skewing

Table 3 Monotonicity of each items with skewing angle

Items	α_e	cosγ	K_{s1}	L_d^{sk*}	L_q^{sk*}	sin2γ	K_α
Monotonicity	↑	✓	↓	↑	↓	✓	↓

Ps: ✓: unchanged; ↑: increase; ↓: decrease.

4 Conclusion

The stator self- and mutual-inductance and synchronous inductance are very important to the drive performance prediction and control strategy implementation of PMSMs. However, when stator skewing is employed to improve the electromagnetic performances, 3D FEA calculations are required to get the inductances requiring significant computational effort and time because of the numerous meshes.

In this paper, an improved hybrid method combining 2D FEA and an analytical method is proposed to estimate the stator winding inductance and

synchronous inductance taking into effect stator skewing influence. In order to verify FEA simulations, extensive experiments are put forward for three IPMSMs, including one normal and two skewed machines (half slot and one slot pitch skewing respectively), showing good correlation with 3D FEA simulations.

Main contributions in this paper can be summarized as follows:

- The proposed method improves the calculation accuracy of the skew influence on the inductances. In general, conventional methods always subdivide the axial length of the skewed machine into several slices and integrate the inductance of each slice together. However, it does not consider the variation of the inductances with the axial position. It is taken into account in this paper by introducing two factors which are related to skewing angle.
- The influences of skewing effect on the inductances are investigated on both SPMSM and IPMSM respectively. The inductances of SPMSM decreases, while for IPMSM, L_d increases and L_q decreases when skewing is employed.

Comprehensive investigations and comparisons are made on the influence of skewing angel on stator self-, mutual- inductances, synchronous inductances, and torque-speed curves for IPMSM. It is found that as skewing angle increases, L_d becomes bigger while L_q goes down, thus reducing the rotor saliency and maximal torque capability in constant power region, but increasing the output torque capability in flux weakening region.

References

[1] L. J. Wu, Z. Q. Zhu, and J. T. Chen, "Optimal split ratio in fractional-slot interior permanent magnet machines with non-overlapping windings," *IEEE Trans. Magn.*, vol. 46, no. 5, pp. 1235-1242, May 2010.

[2] P. Zhou, D. Lin, G. Wimmer, and N. Lambert, "Determination of Axis Parameters of Interior Permanent Magnet Machine," *IEEE Trans. Magn.*, vol. 46, no. 8, pp. 3125-3128, Aug. 2010.

[3] H. V. Xuan, D. Lahaye, and H. Polinder, "Influence of stator slotting on the performance of permanent-magnet machines with concentrated windings," *IEEE Trans. Magn.*, vol. 49, no. 2, pp. 929-938, Feb. 2013.

[4] T. M. Jahns, G. B. Kliman, and Neumann T. W, "Interior permanent-magnet synchronous motors for adjustable-speed drives," *IEEE Trans. Ind. Appl.*, vol. 4, pp. 738-747, Jul. 1986.

[5] B. J. Chalmers, S. A. Hamed, G. D Baines, "Parameters and performance of a high-field permanent-magnet synchronous motor for variable-frequency operation," *IEE Proceedings B (Electric Power Applications)*, vol. 132, no. 3, pp. 117-124, IET Digital Library, 1985.

[6] K. J. Meessen, P. Thelin, J. Soulard, and E. A. Lomonova, "Inductance calculations of permanent-magnet synchronous machines including flux change and self-and cross-saturations," *IEEE Trans. Magn.*, vol. 44, no. 10, pp. 2324-2331, Oct. 2008.

[7] S. Morimoto, M. Sanada, Y. Takeda, "Wide-speed operation of interior permanent magnet synchronous motors with high-performance current regulator," *IEEE Trans. Ind. Appl.*, vol. 30, no.4, pp. 920-926, Jul/Aug 1994.

[8] H. Karmaker, and A. M. Knight, "Investigation and simulation of fields in large salient-pole synchronous machines with skewed stator slots," *IEEE Trans. Energy Conv.*, vol. 20, no. 3, pp. 604-610, Sep. 2005.

[9] M. A. Alhamadi, and N. A. Demerdash, "Modeling of effects of skewing of rotor mounted permanent magnets on the performance of brushless DC motors," *IEEE Trans. Energy Conv.*, vol. 6, no. 4, pp. 721-729, Dec. 1991.

[10] S. Williamson, T. J. Flack, and A. F. Volschenk, "Representation of skew in time-stepped two-dimensional finite-element models of electrical machines," *IEEE Trans. Ind. Appl.*, vol. 31, no.5, pp. 1009-1015, Sep./Oct. 1995.

[11] W. Q. Chu, and Z. Q. Zhu, "Reduction of on-load torque ripples in permanent magnet synchronous machines by improved skewing," *IEEE Trans. Magn.*, vol. 49, no.7, pp. 3822-3825, Jul. 2013.

[12] Bomela X. B., Kamper M. J., "Effect of stator chording and rotor skewing on performance of reluctance synchronous machine," *IEEE Trans. Ind. Appl.*, vol. 38, no.1, pp. 91-100, Jan. 2002.

[13] Z. L. Gaing, C. H. Lin, M. H. Tsai, "Rigorous design and optimization of brushless PM motor using response surface methodology with quantum-behaved PSO operator," *IEEE Trans. Magn.*, vol. 50, no.1, pp. 1-4, Jan. 2014.

[14] M. M. Koo, S. M. Jang, Y. S. Park,"Characteristic analysis of direct-drive wind power generator considering permanent magnet shape and skew effects to reduce torque ripple based on analytical approach," *IEEE Trans. Magn.*, vol. 49, no.7, pp. 3917-3920, Jul. 2013.

[15] M. A. Alhamadi, and N. A. Demerdash, "Modeling and experimental verification of the performance of a skew mounted permanent magnet brushless DC motor drive with parameters computed from 3D-FE magnetic field solutions," *IEEE Trans. Energy Conv.*, vol. 9, no. 1, pp. 26-35, Mar. 1994.

[16] H. De Gersem, K. Hameyer, and T. Weiland, "Skew interface conditions in 2-D finite-element machine models," *IEEE Trans. Magn.*, vol. 39, no. 3, pp. 1452-1455, May 2003.

[17] Y. S. Chen, Z. Q. Zhu, and D. Howe, "Calculation of d- and q-axis inductances of PM brushless ac machines accounting for skew," *IEEE Trans. Magn.*, vol. 41, no.10, pp. 3940-3942, Oct. 2005.

[18] G. Qi, J. T. Chen, Z. Q. Zhu, "Influence of skew and cross-coupling on flux-weakening performance of permanent-magnet brushless AC machines," *IEEE Trans. Magn.*, vol. 45, no. 5, pp. 2110-2117, May 2009.

[19] Tessarolo A., "Accurate computation of multiphase synchronous machine inductances based on winding function theory," *IEEE Trans. Energy Conv.*, vol. 27, no. 4, pp. 895-904, Dec. 2012.

[20] J. Faiz, and I. Tabatabaei, "Extension of winding function theory for nonuniform air gap in electric machinery," *IEEE Trans. Magn.*, vol. 38, no. 6, pp. 3654-3657, Nov. 2002.

[21] H. A. Toliyat, M. M. Rahimian, and T. A. Lipo, "d-q Modeling of five phase synchronous reluctance machine including third harmonic of air-gap MMF," in *Conf. Rec. IEEE-IAS Annu. Meeting*, 1991, pp. 231-237 .

[22] T. Lubin, T. Hamiti, H. Razik, "Comparison between finite-element analysis and winding function theory for inductances and torque calculation of a synchronous reluctance machine," *IEEE Trans. Magn.*, vol. 43, no.8, pp. 3406-3410, Aug. 2007.

[23] J. M. Gojko, D. D. Momir, and O. B. Aleksandar, "Skew and linear rise of MMF across slot modelling-winding function approach," *IEEE Trans. Energy Conv.*, vol. 14, no.3, pp. 315-320, Sep. 1999.

[24] R. Dutta, and M. F. Rahman, "A comparative analysis of two test methods of measuring d- and q- axes inductances of interior permanent-magnet machine," *IEEE Trans. Magn.*, vol. 42, no. 11, pp. 3712-3718, Nov. 2006.

[25] Q. Li, T. Fan, and X. Wen, "Armature-reaction magnetic field analysis for interior permanent magnet motor based on winding function theory," *IEEE Trans. Magn.*, vol. 49, no. 3, pp. 1193-1201, Mar. 2013.

[26] A. Chiba, F. Nakamura, T. Fukao, "Inductances of cageless reluctance-synchronous machines having nonsinusoidal space distributions," *IEEE Trans. Ind. Appl.*, vol. 27, no.1, pp. 44-45, Jan./Feb. 1991.

[27] Liwschitz-Garik M., and Whipple C., *Alternating-Current Machines*. New York: Van Nostrand, 1961.

Yuting Gao was born in China. She received the B.Eng. degree in electrical engineering from Huazhong University of Science and Technology, Wuhan, China, in 2012, where she is currently working toward the Ph.D. degree in the School of Electrical and Electronic Engineering.

Her research interests include the design and analysis of novel permanent-magnet and superconducting synchronous machines.

Ronghai Qu (S'01–M'02–SM'05) was born in China. He received the B.E.E. and M.S.E.E. degrees from Tsinghua University, Beijing, China, in 1993 and 1996, respectively, and the Ph.D. degree in electrical engineering from the University of Wisconsin-Madison, in 2002.

In 1998, he joined the Wisconsin Electric Machines and Power Electronics Consortiums as Research Assistant. He became a Senior Electrical Engineer with Northland, a Scott Fetzer Company in 2002. Since 2003, he had been with the General Electric (GE) Global Research Center, Niskayuna, NY, as a Senior Electrical Engineer with the Electrical Machines and Drives Laboratory. He has authored over 120 published technical papers and is the holder of over 50 patents/patent applications. From 2010, he has been a professor with Huazhong University of Science &Technology, Wuhan, China.

Prof. Qu is a full member of Sigma Xi. He has been the recipient of several awards from GE Global Research Center since 2003, including the Technical Achievement and Management Awards. He also is the recipient of the 2003 and 2005 Best Paper Awards, third prize, from the Electric Machines Committee of the IEEE Industry Applications Society at the 2002 and 2004 IAS Annual Meeting, respectively.

Dawei Li (S'12) was born in China. He received the B.Eng. degree in electrical engineering from Harbin Institute of Technology, Harbin, China, in 2010, and the Ph.D. degree in electrical engineering from Huazhong University of Science and Technology, Wuhan, China in 2015. He is currently a lecturer of the School of Electrical and Electronic Engineering, Huazhong University of Science and Technology, Wuhan, China.

His research interests include the design and analysis of novel permanent-magnet brushless machines.